ACS Catalysis

Research Article

pubs.acs.org/acscatalysis

Ligand Field Effects and the High Spin−High Reactivity Correlation in the H Abstraction by Non-Heme Iron(IV)−Oxo Complexes: A DFT Frontier Orbital Perspective

Andranik Kazaryan and Evert Jan Baerends*

VU University Amsterdam, Theoretical Chemistry, FEW, De Boelelaan 1083, 1081 HV Amsterdam, The Netherlands

Supporting Information

ABSTRACT: The electronic structure explanation of H abstraction from aliphatic CH bonds by the ferryl ion, $Fe^{IV}O^{2+}$, has received a great deal of attention. We review the insights that have been gained, in particular into the effect of the spin state. However, we emphasize that the spin state is dictated by the field of the ligands coordinated to the Fe ion and is but one of the effects of the ligand field. Using the model systems $[FeO(H_2O)_5]^{2+}$, representative of the weak field situation, and $[FeO(H_2O)_{ax}(NH_3)_4]^{2+}$, representative of a strong (equatorial) field, we distinguish the effect of spin state (high spin (quintet) versus low spin (triplet)) from other effects, notably the orbital interaction (pushing up) effect of the ligand donor orbitals and the electron-donating ability of the ligands, directly affecting the charge on the FeO group. We describe the changes in electronic structure during the reaction with the help of elementary orbital interaction diagrams involving the frontier orbitals. These give a straightforward electronic structure picture of the reaction but do not provide support for the description of the reactivity of FeO^{2+} as starting with oxyl radical formation.

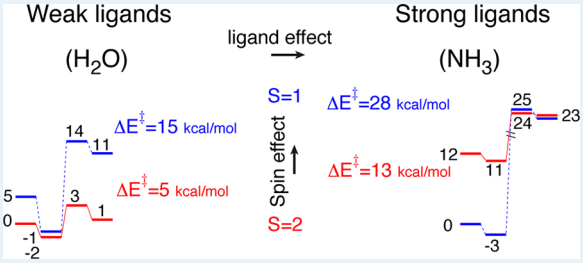

KEYWORDS: *nonheme iron−oxo complexes, oxidation catalysis, DFT calculations, ligand field effects, high-spin low-spin, H abstraction*

INTRODUCTION

High-valent iron−oxo (ferryl, $Fe^{IV}O^{2+}$) compounds have long been considered as active intermediates in the catalytic cycles of heme and nonheme enzymes such as cytochrome P450,[1,2] TauD,[3,4] and MMO[5−7] which catalyze important biological reactions and are capable of hydroxylating inert aliphatic C−H bonds. The ferryl species has also been implicated as the active moiety in abiotic oxidation catalysis, as for example in the Fenton reagent.[8−16] Heme enzymes such as P450, featuring the $Fe^{IV}O^{2+}$ unit in a porphyrinic ring, have been thoroughly studied and the active intermediates, Compounds I and II (Cpd I, Cpd II), were experimentally characterized[17−19] and studied theoretically.[20−27] In nonheme enzymes such as *Escherichia coli* taurine:R-ketoglutarate dioxygenase (TauD),[3] MMO,[5,28−36] and Bacterial Phenylalanine Hydroxylase[37] direct characterization of the ferryl species has also been possible. An abundance of synthetic heme and nonheme Fe^{IV}−oxo compounds have been prepared over the years.[38−40] The majority of synthetic nonheme ferryl compounds possess a low spin (LS) $S = 1$ ground state,[38,39] in contrast to the nonheme ferryl intermediates of the enzymes, which feature $S = 2$ high spin (HS). While the active intermediates of the nonheme enzymes have iron at least partially coordinated with carboxylic oxygens,[39] N coordination with aliphatic amine-based ligands is often employed in the synthetic nonheme reactants,[39,40] because of the higher stability. This is actually the prime cause for the LS character of these compounds: the nitrogen lone pairs are strong donors and, as usual in the HS/LS balance, a strong ligand field induces the LS ($S = 1$) configuration (see refs 41 and 42 and see below. The first high-spin nonheme ferryl synthetic compound was a transient intermediate trapped by Pestovsky et al., which has been assigned to $[FeO(H_2O)_5]^{2+}$.[43] Its HS ($S = 2$) character is in accordance with the weak ligand field of the O coordination.

It has been argued from theoretical work that the HS configuration is favorable for the H abstraction reaction. Solomon,[44,45] de Visser,[46,47] Baerends,[42,48−50] and their co-workers have recognized that the high reactivity of nonheme $S = 2$ compounds is due to the high electrophilicity of the ferryl unit, which efficiently cleaves C−H bonds. The high electrophilicity is due to a low-lying spin-up $\sigma^*\alpha$ (Fe $3d_{z^2}$ − O $2p_z$) empty antibonding orbital that can readily accept an electron from the bonding σ_{CH} HOMO of the CH bond. It has been noted[42,51] that the $S = 2$ spin plays an important role in stabilizing this $\sigma^*\alpha$ orbital due to the exchange field from the four unpaired electrons, which allows it to efficiently interact with the low-lying σ_{CH}. This provides a frontier orbital rationalization of the reactivity of the $S = 2$ compounds. In the $S = 1$ state the $\sigma^*\alpha$ orbital is not sufficiently stabilized and a lower lying spin-down $\pi^*\beta$ orbital (Fe $3d_{xz/yz}$ − O $2p_{x/y}$)

Received: November 2, 2014
Revised: January 13, 2015
Published: January 22, 2015

DOI: 10.1021/cs501721y
ACS Catal. 2015, 5, 1475−1488

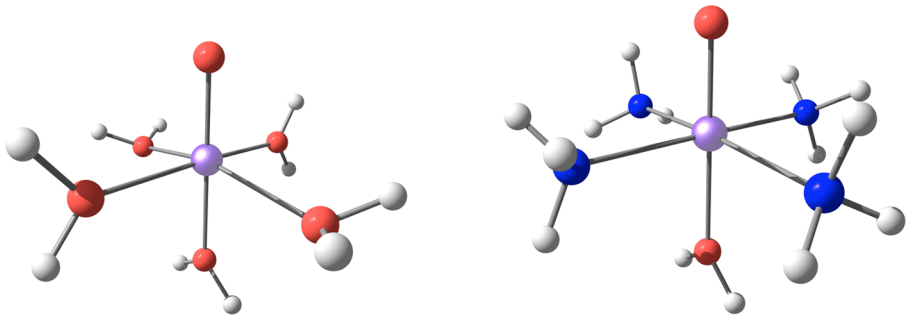

(a) (b)

Figure 1. Structures of the (a) $[FeO(H_2O)_5]^{2+}$ (**1**) and (b) $FeO(H_2O)(NH_3)_4$ (**2**) complexes.

becomes a suitable electron acceptor orbital (EAO).[49,51,52] Reaction via the $\sigma^*\alpha$ orbital is denoted the σ channel, and the reaction via the $\pi^*\beta$ orbital is denoted the π channel. The relative importance of these channels in $S = 2$ and $S = 1$ $Fe^{IV}O^{2+}$ in different ligand environments has been extensively studied.[49,51−55]

The role of the spin states has also been an important issue in the studies on heme compounds. It was shown by Shaik et al.[21,56−58] that the mechanism of H abstraction by a heme Cpd I model involved two spin states (two-state reactivity). These systems have the FeO^{2+} group in the low-spin configuration ($S = 1$), in agreement with the N-donor equatorial environment. The $S = 1$ spin state of FeO^{2+} in Cpd I may then couple with an unpaired electron on the porphyrinic ring system to either quartet or doublet. These couplings do not affect the H abstraction very much. However, in Cpd II there is not an unpaired electron on the porphyrin ring, and the relevant spin states are the $S = 1$ and $S = 2$ states of the FeO^{2+} unit. It has recently been shown[27] that in Cpd II the quintet and triplet states of the FeO^{2+} unit play a role similar to that in the nonheme systems cited above, exhibiting a lower barrier in the $S = 2$ state than in the $S = 1$ state. Since the $S = 1$ state is lower in the reactant complex, due to the N-donor ligands, while the barrier in the quintet state is lower, the $S = 2$ PES crosses toward the transition state (TS) of the low-spin (LS, $S = 1$) surface. This is the same phenomenon observed in the nonheme systems with N-based equatorial ligands.[59,60] Shaik and co-workers[61−63] have given an explanation for lower barriers in high-spin states in the form of the principle of Exchange Enhanced Reactivity (EER): high-spin states will lead to lower barriers by lower electron repulsion caused by energy lowering exchange integral contributions. This favors in the $S = 2$ state the transfer of an α spin electron (from the CH $\sigma\alpha$ bonding orbital to the FeO^{2+} $\sigma^*\alpha$ orbital), so that one more spin-up electron is added to the four that are already present, with concomitant exchange stabilization. This will induce a lower barrier on the quintet surface.

It has also been argued that the role of spin states is best understood in terms of an effective breaking (weakening) of the Fe−O bond en route to the TS, where one electron of the electron pair in an Fe−O bonding orbital (either the 2σ orbital or a π orbital; see below for orbital interaction schemes) localizes on the Fe ion and the opposite spin electron localizes on O. This possibility has been put forward by Solomon and co-workers[45,51,54] in their study of aromatic electrophilic attack by (4-hydroxyphenyl)pyruvate dioxygenase (HPPD) and H abstraction by (4-hydroxy)mandelate synthase (HmaS) and has recently been emphasized by Ye and Neese.[64,65] In the case of the σ channel this means that the $2\sigma\alpha$ orbital becomes predominantly an Fe d_{z^2} orbital, which can be interpreted as the presence of an additional α spin electron on Fe. The Fe ion then can be denoted Fe^{III} d^5, $S = 5/2$. The $2\sigma\beta$ orbital acquires much oxygen character, which is interpreted as the formation of an oxyl radical, antiferromagnetically coupled to Fe(III) in an exchange coupled $Fe^{III}(S = 5/2)\cdot O^{\bullet-}$ system. In the case of the π channel, a Fe−O π bonding orbital exhibits β spin electron localization on Fe, to be described as $Fe^{III}(S = 3/2)$, while the α spin electron localizes on oxygen. Now there is ferromagnetic coupling between Fe($S = 3/2$) and the oxyl radical in the $Fe^{III}(S = 3/2)\cdot O^{\bullet-}$ system, producing again the overall $S = 2$ spin state.[51] The important point in both cases is that the empty (originally antibonding) partner orbital ($3\sigma^*\alpha$ or $\pi^*\beta$) shows opposite localization, i.e. in both cases toward oxygen, so that a strongly oxygen based empty spin-up acceptor orbital is generated. This would for overlap reasons be favorable for the interaction with the $\sigma(CH)$ orbital.

We will review in this paper the arguments concerning the role of the spin states in the iron−oxo-catalyzed H abstraction reaction. However, we wish to stress that the spin state is but one aspect of the electronic structure. It should be recognized that the spin state cannot be treated independently from other ligand field effects. The key ligand effects in nonheme ferryl compounds will be illustrated with the simple model systems $[FeO(H_2O)_{ax}(L_{eq})_4]^{2+}$, where the equatorial ligands are either $L_{eq} = H_2O$ (compound **1**, Figure 1a) or $L_{eq} = NH_3$ (compound **2**, Figure 1b). As indicated above, strongly electron donating ligands generate the strong (equatorial) ligand field that induces a low-spin configuration (**2** has a triplet ground state, whereas **1** has a quintet ground state). A strong ligand field will push up the (nominally) metal based orbitals, which are antibonding with respect to the ligands. This not only induces a low-spin state by the large ligand field splitting but also lowers, irrespective of the spin state, the electron-accepting ability of the low-lying empty orbitals. At the same time these ligands, donating electron charge to the metal center, will also decrease the positive charge on the metal and the iron−oxo group. However, positive charge on that group is important for the lowering of the barrier to H abstraction, since it lowers the energy of the electron acceptor orbital. Charge of course exerts a strong effect anyway,[66] for instance when charged ligands are considered: positive charge lowers the energy of the acceptor orbital. However, the unfavorable charge effect of electron-donating ligands (strong ligand field) is in practice always tied to the LS configuration generated by this type of ligand. We will try to assess the relative importance of, on the one hand, ligand effects (both direct effects from the overlap between ligand and

DOI: 10.1021/cs501721y
ACS Catal. 2015, 5, 1475−1488

Scheme 1. Schematic Picture of the Relevant Frontier Orbital Interactions in the σ Channel (Which Has Spin-Up Frontier Orbitals):[a] (Left) Weak Donor−Acceptor Bonding between the $\sigma\alpha$(CH) Bonding Orbital and the FeO^{2+} $\sigma^*\alpha$ Orbital in the Reactant Complex (RC); (Right) Lengthening of One C−H Bond in the Transition State (TS) Destabilizing the Corresponding σ(CH) Bond Relative to the Other T_2 CH Bonding Orbitals, Bringing It Much Closer to the FeO^{2+} $\sigma^*\alpha$ Orbital, with Which It Has a Greatly Increased Interaction

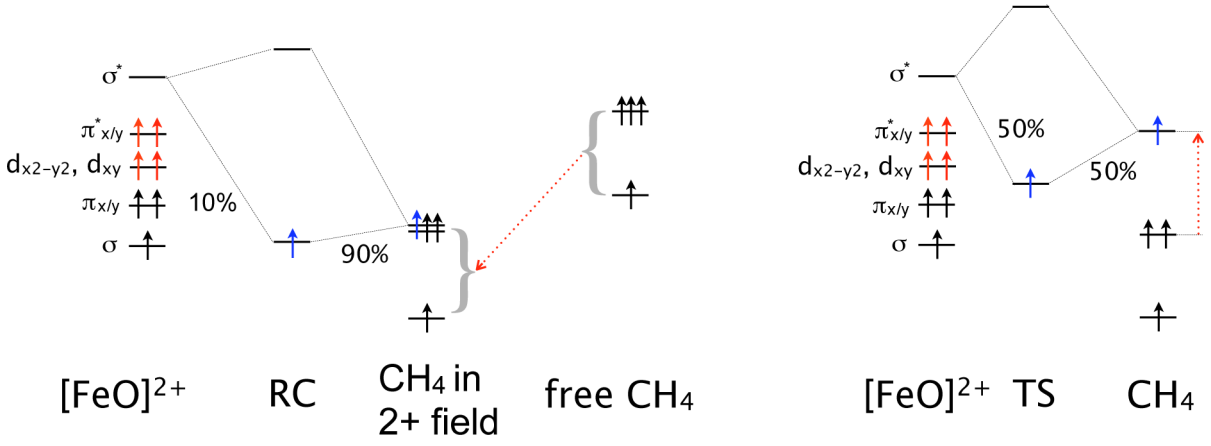

[a]The unpaired electrons on FeO^{2+} are shown in red, and the α spin electron of the σ(CH) bonding orbital that is donated to the FeO^{2+} σ^* is shown in blue. The methane orbitals are stabilized in the complex in comparison to free methane due to the 2+ charge of the metal fragment.

metal orbitals and the indirect effect from charge buildup) and, on the other hand, the spin effect by studying theoretically situations such as a HS configuration in a strong ligand field and a LS configuration in a weak ligand field, which will not readily be found in real systems.

METHODS

All calculations were performed with the Amsterdam Density Functional (ADF) package.[67−69] Unless otherwise noted, the QZ4P basis set was employed for the iron atom and TZ2P for the other atoms (ADF uses Slater type orbitals (STOs), QZ (TZ) stands for quadruple (triple) STO basis for s, p, d valence orbitals, and *n*P indicates *n* sets of polarization functions). Relativistic effects are taken into account through the zero-order regular approximation (ZORA).[70] Since one of the goals of the present study is a comparison of potential energy barriers in the S = 1 and S = 2 states in nonheme ferryl compounds, a density functional is required that will not underestimate the S = 2 energy, which might lead to a dubious conclusion about the increased reactivity in high-spin compounds. In a recent benchmark study, Chen, Lai, and Shaik studied in particular the energetics of H-abstraction by the $[FeO(NH_3)_5]^{2+}$ complex in both S = 1 and 2 states.[62] They compared high-level RCCSD(T) data with various density functionals. From their results it is clear that energies obtained by pure GGA functionals (such as, for example, BLYP and OPBE) are closest to the respective RCCSD(T) in both spin states. Since our systems strongly resemble the $[FeO(NH_3)_5]^{2+}$ compound, we feel confident that the reported benchmark results carry over to our case. We have therefore chosen the BLYP[71,72] exchange-correlation functional for geometry optimization and energy evaluations. Additional B3LYP[71−73] calculations have been carried out (e.g., for the Hirshfeld charge analysis) for verification purposes. Given the strong spin polarization, all calculations were performed with the spin-unrestricted formalism.

To study the orbital structure, we performed fragment analysis as implemented in the ADF program. The molecules were divided into three fragments: iron−oxo moiety, ligands, and the substrate (methane). The fragment analysis has been performed at all geometries along the reaction path, which allowed us to study the evolution of the orbital gross populations and thereby track the electron transfer.

The transition states were located and characterized with a single imaginary frequency. The frequencies are reported in Table S2 in the Supporting Information. Using the transition states, intrinsic reaction coordinate (IRC) scans have been performed.

RESULTS AND DISCUSSION

Spin and Ligand Field Effects. The frontier orbital description of the reactivity of nonheme ferryl compounds in the methane H abstraction by $[FeO]^{2+}$ is summarized in Scheme 1. In this scheme the case of the σ channel is depicted, with only the active spin-up orbitals shown, but a similar scheme would hold in the case of the π channel, in that case with β spin orbitals involved in the relevant orbital interactions. In Scheme 1 the d_{z^2}-based antibonding σ^* orbital plays the role of the electron acceptor orbital (EAO) for the methane bonding HOMO (the electron donor orbital, EDO). In the reactant complex (RC), the methane orbitals become stabilized, in comparison to free CH_4, due to the electrostatic field of the dication. The methane HOMO is quite low in energy (ca. −17 eV: BLYP) with respect to the $\sigma^*\alpha$ orbital (ca. −14 eV: BLYP). Therefore, the methane hydrogen atom forms a weak dative bond (ca. 3 kcal/mol bonding) with the oxygen through a slight- mixing of the σ^* (10%) and σ_{CH} orbitals (90%). Upon stretching of one of the C−H bonds, the triple degeneracy of the C−H methane orbitals is lifted and the σ_{CH} HOMO rises in energy. At the transition state (TS) the HOMO becomes ca. 1 eV higher than the other two $1t_2$ bonding orbitals, and due to a better energy match and overlap with σ^* these orbitals mix strongly, leading to a strong covalent O−H bond. This is a prototypical case of the reduction of the bond breaking energy, which is quite high in the case of methane (106 kcal/mol), through the catalytic effect of a second reagent: in the presence of the ferryl ion the barrier becomes only ca. 5 kcal/mol. As depicted in Figure 2, the stabilization due to the formation of

DOI: 10.1021/cs501721y
ACS Catal. 2015, 5, 1475−1488

the O−H bond increases greatly when the C−H bond is lengthened, providing a large lowering of the barrier.[50]

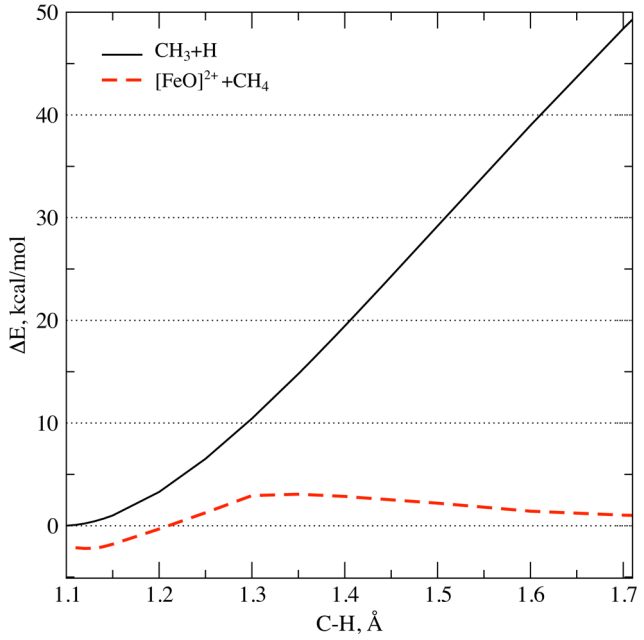

Figure 2. Comparison of the energy required to stretch (and eventually break) a C−H bond in CH_4 and the actual energy profile of the C−H bond stretching in the reaction with the FeO^{2+} group in $[FeO(H_2O)_5]^{2+}$-CH_4.

The orbital energy of the EAO, which obviously is a crucial feature of the electronic structure, is determined by the ligand field through the factors mentioned in the Introduction. The key ligand effects in nonheme ferryl compounds can be illustrated with the simple model systems **1** (Figure 1a) and **2** (Figure 1b). These are pseudo-octahedral d^4 compounds, where the NH_3 ligands yield a strong equatorial ligand field, whereas the H_2O ligands represent the weak-field situation. In an octahedral field we expect splitting of the d levels in a high-lying e_g pair (d_{z^2}, $d_{x^2-y^2}$) and a low-lying t_{2g} set (d_{xz}, d_{yz}, d_{xy}). These splittings are considerably modified by the deviations of the ligand field from octahedral symmetry and by the spin polarization effects. The actual situation is depicted in Figure 3, where the orbital energies for both the spin-up and spin-down levels are shown. The manifold of oxygen 2p and metal 3d orbitals is shown. The lowest levels in the diagram are the 2σ and $\pi_{x,y}$ orbitals. Although in a simple ligand field picture these would be denoted as the O 2p or ligand levels, they are actually rather covalent bonding combinations of O 2p and Fe 3d orbitals. They are doubly occupied, although the α spin orbitals are at considerably lower orbital energies than the β spin counterparts due to the stabilizing exchange field of the excess α spin electrons. The splitting of the d orbitals shows that the field differs considerably from octahedral. The d_{z^2} based $3\sigma^*$ orbital (actually a strong antibonding combination of d_{z^2} and O $2p_z$) is considerably higher than $d_{x^2-y^2}$, which is only pushed up, as usual, by σ antibonding with equatorial ligands. The Fe−O_{oxo} bond is not a typical coordinative bond; it is much shorter and stronger due to the covalent bonds represented by the 2σ and $\pi_{x,y}$ orbitals, and accordingly the antibonding in the (empty) $3\sigma^*$ is stronger than the typical coordinative antibonding of the equatorial ligands with $d_{x^2-y^2}$. For the same reason the $\pi_{x,y}^*$ pair (nominally "metal orbitals" $d_{xz,yz}$ but in fact the antibonding Fe $3d\pi$−O $2p\pi$ partner of the bonding π orbitals) is strongly destabilized and, although of low-lying t_{2g} type in a perfect octahedral ligand field, now is much higher than the remaining t_{2g} level, d_{xy}. It gets close to the e_g type $d_{x^2-y^2}$ (sometimes above, sometimes below). As can be seen in Figure 3, these observations hold for both the α and β spin manifolds.

We can now compare the effects of spin symmetry (quintet versus triplet) and of ligand fields. Due to the strong exchange field of the excess spin-up electrons, the orbital energies of the spin-up levels are considerably lower than for the spin-down levels. The stabilizing exchange field is stronger for the quintet, with four excess α electrons, than for the triplet with only two unpaired α electrons (the unpaired electrons are distinguished by red arrows). Indeed, the $3\sigma^*$ acceptor orbital is, in the pentaaquo complex, at −13.8 and −12.6 eV in the quintet and triplet, respectively. Whether the quintet or triplet is the ground state is governed by the relative energies of the $d_{x^2-y^2}\alpha$ and $d_{xy}\beta$ orbitals. The relevant electron configurations are $(\pi x^*\alpha)$-$(\pi_y^*\alpha)(d_{xy}\alpha)(d_{x^2-y^2}\alpha)$ (quintet) and $(\pi x^*\alpha)(\pi_y^*\alpha)$-$(d_{xy})^2(d_{x^2-y^2})^0$ (triplet). Occupying $d_{x^2-y^2}$ with a majority spin electron instead of doubly occupying d_{xy} is favorable because of exchange stabilization, but as always in HS/LS couples, when the one-electron energy of the $d_{x^2-y^2}\alpha$ level would become too high (which we will see happen with the strongly pushing equatorial NH_3 ligands) the energy penalty of occupying the orbital becomes too high, and the electron will "fall down" in the lower lying d_{xy} orbital in spite of the necessary spin pairing. In the case of equatorial water ligands the field is sufficiently weak so that $d_{x^2-y^2}\alpha$ becomes occupied in the ground state, which is then a quintet state.

In the ammoniated compound $FeO(H_2O)(NH_3)_4$, again $3\sigma^*\alpha$ is ca. 1 eV lower in the quintet state (−12.3 eV) than in the triplet state (−11.2 eV). More importantly, however, the $3\sigma^*$ levels are ca. 1.4−1.5 eV higher than in the corresponding aquo complex. This upshift has two sources. Strong ligands have a stronger pushing-up effect on overlap grounds (larger overlap with metals and/or higher lying ligand level). This implies also stronger electron donation to the metal (or in this case the iron−oxo moiety), which thus becomes less positive. This charge effect enhances the upshift of the metal orbitals and also affects "inert" metal orbitals that have little or no overlap with the ligand orbitals. We will discuss below to what extent the "orbital overlap effect" and the "charge effect" can be distinguished. We note that the ligand effect on the orbital energies (change from water to ammonia equatorial ligands) is even larger than the spin effect (change from quintet to triplet). However, with strong ligands these effects add up: strong equatorial ligands push $d_{x^2-y^2}\alpha$ up so much that the *triplet* becomes the ground state. This has an additional adverse effect on the reactivity (in the σ channel), since the $3\sigma^*\alpha$ acceptor orbital has higher energy in the triplet. This "spin effect" of ca. 1.1 eV (in the ammoniated system) is caused by the strong ligand field generating a triplet ground state and therefore inevitably occurs in conjunction with the other ligand effects on the orbital energies already mentioned. We will quantify the magnitude of these qualitative frontier orbital trends on the energies of the transition state barriers in the next section.

Transition State Barriers. Scheme 2 presents the energies of the reactant complexes (RC), the transition states (TS), and the product complexes (PC)[94] for both $[FeO(H_2O)_5]^{2+}$ (**1**) and $[FeO(H_2O)(NH_3)_4]^{2+}$ (**2**). The spin effect is clear from the lower TS energy, for a given compound (ligand environment), on the quintet surface than on the triplet

DOI: 10.1021/cs501721y
ACS Catal. 2015, 5, 1475−1488

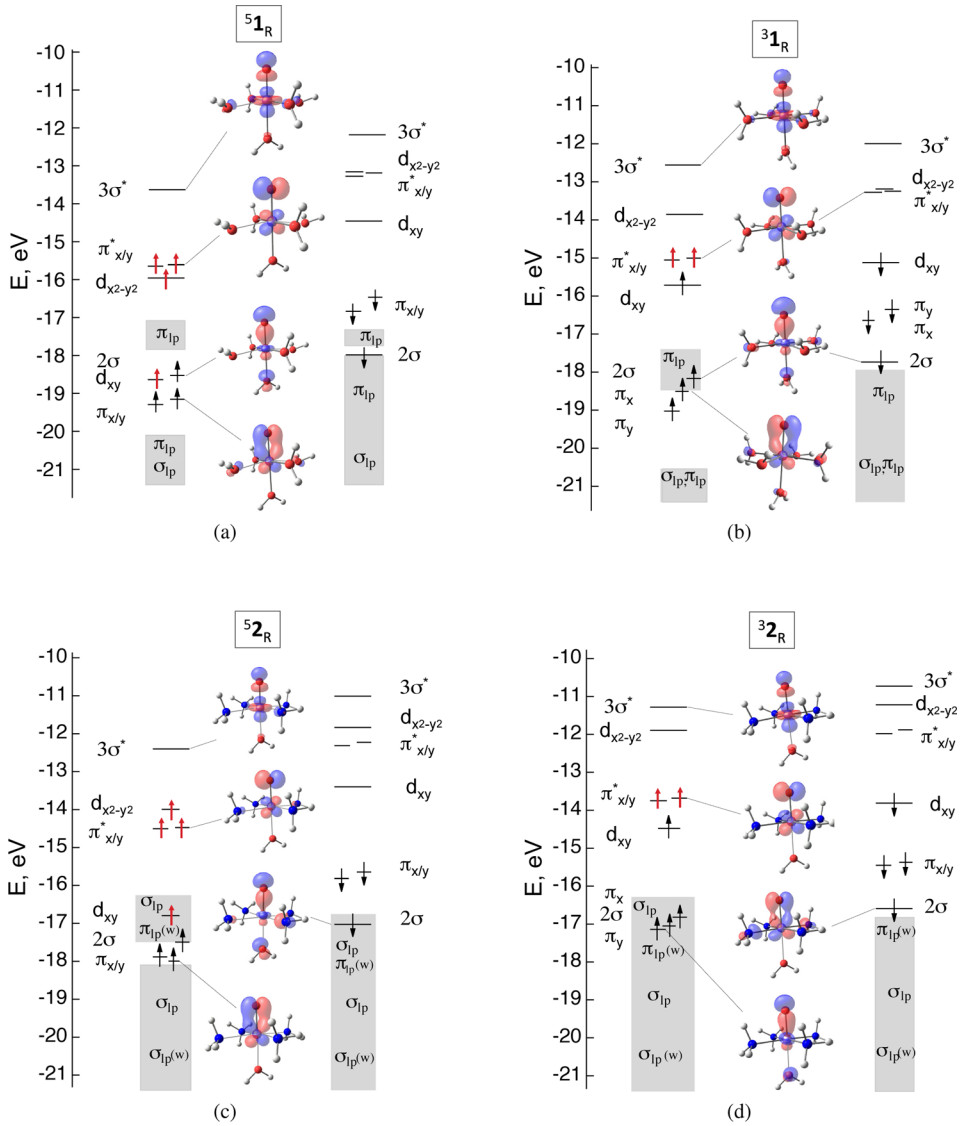

Figure 3. Frontier Kohn–Sham orbitals of the free reactants $[FeO(H_2O)_5]^{2+}$ with (a) $S = 2$ ($^5\mathbf{1}_R$) and (b) $S = 1$ ($^3\mathbf{1}_R$) and of $[FeO(H_2O)(NH_3)_4]^{2+}$ with (c) $S = 2$ ($^5\mathbf{2}_R$) and (d) $S = 1$ ($^3\mathbf{2}_R$) (subscript R denotes the reactant, and the unpaired electrons are shown in red). In each panel the α spin orbitals are to the left and the β spin orbitals to the right. The orbitals are denoted according to the predominant FeO^{2+} fragment orbital in the orbital of the complex.

surface: 3.3 kcal/mol for quintet versus 8.6 kcal/mol for triplet in **1** and 11.4 kcal/mol for quintet versus 24.8 kcal/mol for triplet in compound **2**. This is in accordance with the trends in frontier orbital energies noted in the previous section. We will see below that the actual orbital involvement is more complicated than is assumed there; sometimes the barrier can be lowered by the oxidant (also) using an orbital other than $3\sigma^*$, but that can apparently not break the predicted trend. In **1** there is no crossing of energy surfaces of different spin; the reaction can completely proceed on the HS surface. In system **2**, which is, with its N donor equatorial ligands, more analogous to the many synthesized nonheme iron–oxo compounds, the triplet ground state lies considerably lower than the quintet (by 12.3 kcal/mol), but due to the much lower barrier on the quintet surface the quintet TS energy is still lower than the triplet TS energy. This is the typical cutting of the quintet surface through the triplet surface that has been extensively discussed for the nonheme ironoxo compounds with equatorial N donor ligands which were synthesized as P450 mimics.[57−60,74] In the P450 systems[21,56] the focus has been on the lower lying triplet state of FeO^{2+}, which could couple to an unpaired electron on the porphyrin ring in Cpd I to give a doublet or quartet; the quintet FeO^{2+} derived quartet and sextet are too high-lying to play a role. In Cpd II, with a close-shell Por^{2-} ring, the cutting of the quintet surface through the triplet surface does happen.[27] However, an important theme of the present paper is that not just the spin effect is important but in particular the ligand effect is strong. In **2** both barriers are higher than the corresponding barriers in **1**: the quintet barrier goes up more strongly by changing the H_2O ligands for NH_3 ligands (from 3.3 to 11.4 kcal/mol) than by going to the triplet with unchanged ligands (from 3.3 to 8.6 kcal/mol). For the triplet barrier the ligand effect (i.e., going from 8.6 kcal/mol in $^3\mathbf{1}$ to 24.8 kcal/mol in $^3\mathbf{2}$) is much stronger than any spin effect.

Before considering in more detail the origin of the ligand effect, we will first discuss some of the electronic structure features of this reaction.[13,29,42,45,47−50,52,55,58,63,64,75−79] An excellent comprehensive discussion has recently been given

DOI: 10.1021/cs501721y
ACS Catal. 2015, 5, 1475−1488

Scheme 2. Energies (in kcal/mol) of the Reactant Complexes, Transition States, and Product Complexes of the Methane H Abstraction Reactions by the Oxidants $FeO(H_2O)_5^{2+}$ (1, Left) and $FeO(H_2O)(NH_3)_4^{2+}$ (2, Right) in Quintet and Triplet States[a]

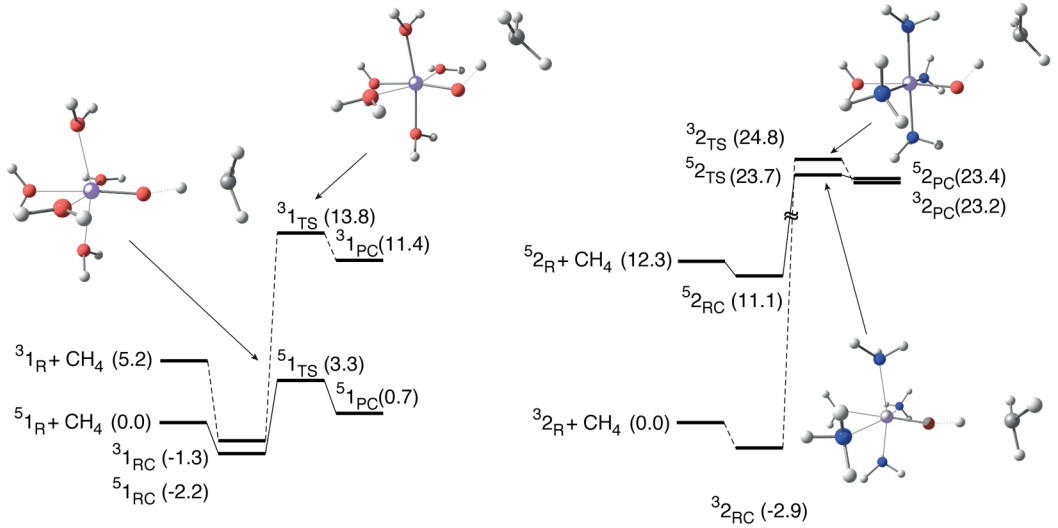

[a]The energies are with respect to the ground state free reactants. The ground state of compound **1** is a quintet, and that of compound **2** is a triplet. Note that the product complex PC is not the product complex of the complete hydroxylation reaction, which would also include the O rebound step.

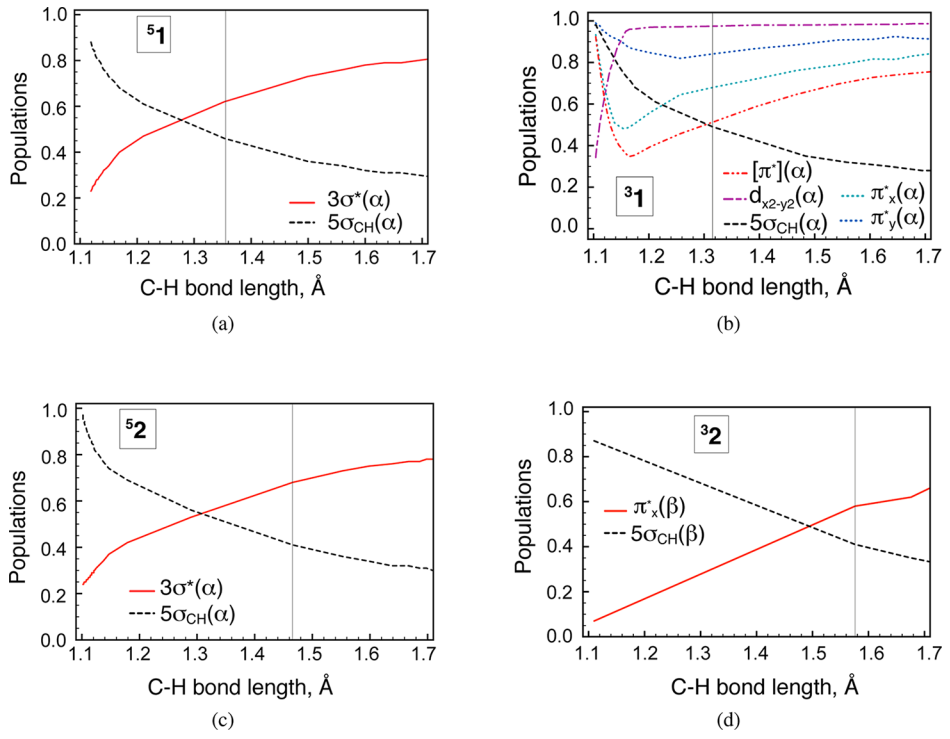

Figure 4. Gross orbital populations of orbitals of the fragment FeO^{2+} along the intrinsic reaction coordinate (projected on the C−H bond length) in H abstraction from methane by $[FeO(H_2O)_5]^{2+}$ with (a) $S = 2$ (^{5}**1**) and (b) $S = 1$ (^{3}**1**) and by $[FeO(H_2O)(NH_3)_4]^{2+}$ with (c) $S = 2$ (^{5}**2**) and (d) $S = 1$ (^{3}**2**). Vertical lines indicate the transition state. The acceptor orbitals (σ^* or π^*) become populated during the reaction, whereas the methane HOMO donor orbitals σ_{CH} lose an electron. In the case of ^{3}**1** (b) one of the two initially occupied $\pi^*\alpha$ orbitals becomes the acceptor orbital. Because of the degeneracy, the effective population of the acceptor orbital is estimated as $[\pi^*]\alpha = \pi_x^*\alpha + \pi_y^*\alpha - 1$.

by Ye, Geng, Shaik, and Neese in ref 80. The quintet of compound **1** ($FeO(H_2O)_5$) (denoted ^{5}**1**) and the triplet of compound **2** ($FeO(H_2O)(NH_3)_4$) (denoted ^{3}**2**) are the typical cases which have received much attention in the literature. In ^{5}**1** $3\sigma^*\alpha$ is the lowest empty electron acceptor in the manifold of the α spin orbitals. Among the β spin orbitals the empty $d_{xy}\beta$ is lower in energy (see Figure 3a), but this orbital cannot overlap with a reactant, being shielded by the ligands. The $\pi^*\beta$ orbitals are low enough in energy to become involved. However, in order to build up good overlap with a $\pi^*\beta$ orbital, i.e. with the O $2p_x$ or O $2p_y$ content of that orbital, the methane σ(CH) bonding orbital should approach the oxo group sideways. This cannot be done without generating steric repulsion with the equatorial ligands. It turns out that in the TS geometry of ^{5}**1** (see the insets in Scheme 2 and see the key geometric parameters in Table S2 in the Supporting Information) the

DOI: 10.1021/cs501721y
ACS Catal. 2015, 5, 1475−1488

methane approach is linear; thus, apparently the σ channel prevails in this case. In Figure 4a the development of the gross populations of the $\sigma^*\alpha$ and the $\sigma(CH)\alpha$ orbitals are given as a function of the reaction coordinate (projected here on the C−H bond length). This illustrates the depletion of the $\sigma(CH)\alpha$ orbital and occupation of the $\sigma^*\alpha$ orbital along the reaction coordinate in the quintet compounds, in complete accordance with the proposed electronic structure picture of increasing donation out of the (lengthening) C−H bond into the $\sigma^*\alpha$ acceptor orbital. (We use in Figure 4 orbitals such as σ^* and $\pi_{x,y}^*$ of the FeO^{2+} fragment; the similarly denoted orbitals of the complexes **1** and **2** in Figure 3 consist predominantly of these FeO^{2+} orbitals.)

Turning to the triplet of the ammoniated compound ^{3}**2**, it should be noted that the orbital levels have considerably changed (see Figure 3d): the σ^* orbital is now clearly above the $\pi^*\beta$ orbitals, so that these could become competitive acceptor orbitals (the (now) empty $d_{x^2-y^2}$ is the LUMO in the manifold of α orbitals, but it is not accessible to the approaching methane and is in fact still slightly above $\pi^*\beta$). The inset in Scheme 2 and the geometric parameters (in Table S2 in the Supporting Information) show that the FeOH angle approaches 120°; thus, the methane apparently tries to use one of the $\pi^*\beta$ orbitals as an acceptor orbital. This is a pattern that is well-known in the H abstraction in the P450 type Cpd I,[1,45,46,52,64,75,77,78] in which the FeO^{2+} is in the triplet state, being equatorially surrounded by the N donors of the porphyrin ring system. The role of the $\pi^*\beta$ orbital is confirmed in Figure 4d, which shows that indeed electron transfer takes place from the $\sigma(CH)\beta$ to the $\pi_x^*\beta$ orbital in the course of the reaction (the $\sigma(CH)$ orbital of methane approaches the xz plane).

We have also investigated theoretically the two cases where the systems are in the excited spin states: the ^{3}**1** and the ^{5}**2** systems. System **2** mimics a porphyrin ligand environment (four equatorial N donors) that has been studied in the context of the reactivity of the P450 compounds.[20,21,27,56,81] In Cpd I, however, the quintet is too high lying and the triplet FeO^{2+} has been the focus of interest, and the two spin states of interest (doublet and quartet) arise from coupling of this triplet to the unpaired electron on the porphyrin ring. It is only in Cpd II, with a closed-shell Por^{2-} ring, that the cutting of the FeO^{2+} quintet based surface through the triplet surface does happen.[27] This is what we saw also for our model system **2** in Scheme 2. We also observe that the approach of methane in the ^{5}**2** TS is linear (see inset of Scheme 2), in accordance with a picture where the σ^* is the acceptor orbital, so that methane seeks maximum overlap with this orbital. This is confirmed in Figure 4c, where we see that the $\sigma(CH)\alpha$ orbital is losing its population to $\sigma^*\alpha$. The frontier orbitals of ^{5}**2** in Figure 3c show that $\sigma^*\alpha$ is indeed a suitable acceptor orbital: it is very slightly lower than $\pi^*\beta$ and will be preferred on the ground of favorable overlap and less steric repulsion upon the linear approach of methane. Being a quintet system with the typical σ pathway for the quintet reaction does however not necessarily mean that the TS barrier is low: it is much higher than for the ^{5}**1** system, on account of what we called the ligand effect.

Turning to the ^{3}**1** system, it appears this is not simply mirroring the prototypical triplet behavior of going by way of a $\pi^*\beta$ channel (as in the case of ^{3}**2**). The approach of methane is at ca. 120° (see inset of Scheme 2), which indicates the involvement of a π^* orbital. However, it is not a $\pi^*\beta$ but a $\pi^*\alpha$ orbital in this case. In the ^{3}**1** system we have the somewhat special situation that the empty $d_{x^2-y^2}\alpha$ is rather low-lying, considerably below $\sigma^*\alpha$ (see Figure 3b). The empty $\pi^*\beta$ orbitals are clearly at higher energy, whereas the occupied $\pi^*\alpha$ orbitals are not much below the empty $d_{x^2-y^2}\alpha$. This orbital energy pattern is just a consequence of the electronic nature of the H_2O ligands, which are weak σ donors that do not destabilize $d_{x^2-y^2}\alpha$ strongly, and which are also weak π donors that push π^* up somewhat. The system can easily excite a $\pi^*\alpha$ electron to the "spectator" $d_{x^2-y^2}\alpha$, thereby offering the incoming methane $\sigma(CH)\alpha$ orbital a low-lying $\pi^*\alpha$ acceptor orbital. This is equivalent to a relief of Pauli repulsion: the $\sigma(CH)\alpha$ orbital will make bonding and antibonding combinations with the low-lying $\pi^*\alpha$ in the plane of the O−H−C atoms, and if the antibonding combination remains occupied this implies Pauli repulsion. The antibonding combination rises in energy, and when it becomes higher than the "inert" $d_{x^2-y^2}$ orbital, it can shed its electron into the $d_{x^2-y^2}$ orbital, which removes the Pauli repulsion and only leaves the favorable interaction in the bonding orbital between $\pi^*\alpha$ and $\sigma(CH)\alpha$. This $\pi^*\alpha$ channel has the advantage over the $\pi^*\beta$ channel which is observed in ^{3}**2** that an α spin electron is transferred to the FeO moiety, which can benefit from the exchange stabilization with the two unpaired α spin electrons already present (EER). The electron transfer processes can be followed in the population evolution (Figure 4b). The gradual diminishing of the $\sigma(CH)\alpha$ population is analogous to the other cases, but the other population changes in the initial stages of the reaction are special. It can be seen that the initially almost vacant (0.3e) $d_{x^2-y^2}\alpha$ orbital gains 0.7e already at C−H = 1.15 Å, well before the TS at 1.316 Å (BLYP). (The initial 0.3e in the FeO^{2+} $d_{x^2-y^2}\alpha$ orbital comes from the donation by the ligand lone pairs into the $FeO(H_2O)_5^{2+}$ complex. This donation is visible because we use in Figure 4b the orbitals $d_{x^2-y^2}\alpha$ and $\pi^*\alpha$ of the FeO^{2+} fragment, not the similarly denoted orbitals (because they predominantly have this FeO^{2+} orbital character) of the complexes **1** and **2** in Figure 3.) Simultaneously the FeO^{2+} $\pi^*\alpha$ orbitals lose together 0.7e. Thus, at C−H = 1.16 Å $d_{x^2-y^2}\alpha$ is fully occupied, whereas a $\pi^*\alpha$ becomes a suitable acceptor orbital. Beyond C−H = 1.16 Å we see the "normal" pattern where the occupation of the $\pi^*\alpha$ acceptor orbital rises, while $5\sigma\alpha$(CH) is depopulated.

The description we have given of the electronic structure features of the reaction is reflected in the behavior of the Fe−O bond length (see Figure 5). It is clear that the donation of charge into the antibonding orbitals of either $\sigma^*\alpha$ character (in

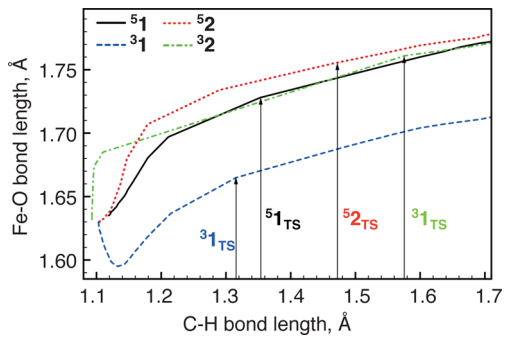

Figure 5. Evolution of the iron−oxo bond length along the reaction coordinate (C−H bond length) in the H abstraction from methane by $[FeO(H_2O)_5]^{2+}$ (**1**) and $[FeO(H_2O)(NH_3)_4]^{2+}$ (**2**). The reaction coordinate values corresponding to the various transition states are indicated with arrows.

DOI: 10.1021/cs501721y
ACS Catal. 2015, 5, 1475−1488

Table 1. Hirshfeld Charges of the Iron−Oxo Moiety and Ligands in Compounds $[FeO(H_2O)_5]^{2+}$ (1) and $[FeO(H_2O)(NH_3)_4]^{2+}$ (2) in Quintet and Triplet States[a]

	q(1)		q(2)		q(1) − q(2)	
spin	FeO	ligands	FeO	ligands	FeO	ligands
S = 2	1.40 [1.46]	0.61 [0.54]	1.30 [1.37]	0.70 [0.63]	0.09 [0.09]	−0.09 [-0.09]
S = 1	1.28 [1.34]	0.72 [0.66]	1.18 [1.23]	0.82 [0.77]	0.10 [0.11]	−0.10 [-0.11]

[a]The positive difference between FeO charges in compounds **1** and **2** demonstrates that a stronger ligand environment (such as NH_3) donates negative charge to the FeO moiety. The results were obtained using BLYP and B3LYP (in brackets) exchange-correlation functionals.

the linear methane approaches in the quintet systems) or into $\pi^*\beta$ (in the 120° approach in ^{3}**2**) leads to lengthening of the Fe−O bond, although we observe, for future reference, that these lengthenings are quite modest up to the TS. The ^{3}**1** system is the odd one out: it starts with a *shortening* of the FeO bond, in agreement with the depopulation of the antibonding $\pi^*\alpha$ orbitals, during the initial transfer of an electron to the nonbonding $d_{x^2-y^2}\alpha$. After this transfer, the normal pattern becomes visible of elongation of the Fe−O bond upon gradual donation of electronic charge out of the $\sigma(CH)\alpha$ orbital of methane into a $\pi^*\alpha$ orbital.

In the foregoing we quantified the effect of the ligand field and of the spin state on the EAOs and on the resulting energy barriers. However, the situation is complicated by the difference of the reaction channels and the EAOs. To assess the contributions to the energy barrier, we carried out an energy decomposition analysis. In order to draw a clear-cut conclusion, we, in addition, considered constrained models whereby only a σ channel is utilized and therefore the EAO is in each case the $3\sigma^*$ orbital. In this fashion we were able to single out the spin and ligand effects on the orbital interaction contribution to the energy barrier. This confirmed our findings for the unconstrained systems. The details of the energy decomposition analysis are given in the Supporting Information.

Summarizing, the electronic structure study of the hydrated and equatorially ammoniated ferryl systems in the $S = 1$ and $S = 2$ states demonstrates the following. (i) For a given spin state, strong equatorial ligands lead to a considerable increase in the barrier, in both the triplet and quintet states (the ligand effect); this is due to a destabilization of the metal−ligand antibonding acceptor orbitals (σ^* or π^*) in the reaction. (ii) For a given set of ligands, the high-spin state leads to a lower barrier than the low-spin state. This can be rationalized in a frontier orbital description as resulting from additional exchange stabilization in the high-spin state of the acceptor orbital (the σ^* orbital in the case of the quintet states). Since strong ligands induce low-spin ground states, this is a second reason strong ligands lead to a high barrier. (iii) In the $S = 2$ states $\sigma^*\alpha$ is the acceptor orbital, whereas in the $S = 1$ state a π^* orbital becomes the acceptor orbital. If in the $S = 1$ state the $\pi^*\beta$ orbital is the acceptor orbital, as in ^{3}**2**, the electron that is transferred is a minority spin electron, and the TS cannot benefit from the exchange stabilization by an additional majority spin electron, as in the EER mechanism; If in the $S = 1$ state the $\pi^*\alpha$ orbital is the acceptor orbital, as in ^{3}**1**, the electron that is transferred is a majority spin electron, and the TS *can* benefit from the exchange stabilization by an additional majority spin electron (EER); note that the EER in this case applies in the low-spin situation.

Charge Distribution and Ligand Effect. Ligands exert their effect directly by way of overlap with metal orbitals, the orbital interaction then leading to pushing up or pushing down of orbitals. These orbital interactions are of course inevitably connected with charge transfers, which will also affect "inert" orbitals that overlap little or not at all with ligand orbitals. Table 1 gives the Hirshfeld charges, which show that the iron−oxo unit is more positive in the hydrated (**1**) compound whereas the ligands are more positive in the ammoniated compound **2**. This is in agreement with the stronger electron donating capability of the ammonia ligands. These charge shifts can help us explain the trends in the orbital energies of the acceptor orbitals, the σ^* and π^* orbitals. The $\sigma^*\alpha$ orbitals of ^{5}**2** and ^{3}**2** are both destabilized (by 1.0 and 1.4 eV, respectively) with respect to the $\sigma^*\alpha$ orbital of the corresponding quintet and triplet aquo compounds. The σ type interaction of the N lone pairs of ammonia with the torus of the d_{z^2} orbital will be partially responsible for this but can be expected to be considerably weaker than the N lone pair interaction with $d_{x^2-y^2}$. To obtain an estimate of the indirect ligand effect (the charge effect), one can refer to the $\pi^*\alpha$ orbitals, since the latter do not interact with the N lone pairs because of symmetry. It is evident from Table S1 (in the Supporting Information) that the π^* orbitals are also destabilized by 1.1 eV (in the quintets) or 1.3 eV (in the triplets). This destabilization can not be explained in terms of a stronger repulsive orbital interaction with the NH_3 ligands; thus, it is a clear sign of the importance of the reduction of the positive charge of the iron−oxo moiety due to a stronger donation from the ammonia ligands. In fact, it appears that the destabilization of $\sigma^*\alpha$ in the ammoniated compound **2** in comparison to the aquo compound **1** is mostly an indirect (charge) effect. If we compare the $d_{x^2-y^2}$ orbital in the ammoniated compound with that in the aquated compound, we note that the difference is ca. 2 eV in the triplets (^{3}**2** at −11.9 eV in comparison to ^{3}**1** at −13.9 eV) and the same in the quintets (^{5}**2** at −13.9 eV in comparison to ^{5}**1** at −15.9 eV). This is considerably more than the 1.1−1.3 eV that could come from the charge effect, in keeping with the expected stronger pushing up by the N lone pairs of the NH_3 ligands.

Spin Densities and Electronic Structure Description of the Reaction. The active moiety in the reaction we are studying is the $Fe^{IV}O^{2+}$ unit, which has many unpaired spins. Indeed, the presence of unpaired spins in metal−oxo clusters and the possible role in their reactivity in H abstraction reactions, or hydrogen atom transfer (HAT) in general, has been highlighted by Schwarz and co-workers.[82] Recently, there has been considerable interest in the suggestion that the H abstraction reaction with $Fe^{IV}O^{2+}$ proceeds via the formation of an oxyl radical antiferromagnetically coupled to a high-spin ($S = 5/2$) Fe ion or ferromagnetically coupled to an intermediate-spin ($S = 3/2$) Fe ion.[45,51,54,64,65] The changes in electronic structure upon stretching the Fe−O bond to the TS value are interpreted as formation of an oxyl radical. We consider here some electronic structure aspects of the reaction, including the spin density developments in the reactants and the oxyl radical picture.

DOI: 10.1021/cs501721y
ACS Catal. 2015, 5, 1475−1488

The electronic structure aspects of the reaction up to the TS can be described very simply with the help of elementary orbital interaction diagrams. In the σ channel approach in ^{5}**1**, for instance, the orbital energies of the free reactant of Figure 3a indicate that the main expected interaction will be that of the occupied $\sigma(CH)\alpha$ with the empty $3\sigma^*\alpha$. Rosa and Ricciardi[27] have emphasized that the additional possibility of interaction with the occupied $2\sigma\alpha$ orbital is important and should be taken into account. Because $2\sigma\alpha$ and $\sigma(\mathrm{CH})\alpha$ are both occupied, this implies Pauli repulsion between these α-spin electrons (half of the repulsive interaction that is commonly called a two-orbital four-electron interaction in the case of closed shells). One way to view the total three-orbital interaction ($2\sigma\alpha$, $\sigma(\mathrm{CH})\alpha$, and $3\sigma^*\alpha$) is as Pauli repulsion between $2\sigma\alpha$ and $\sigma(\mathrm{CH})\alpha$ in a first step, which drives the antibonding combination of these orbitals up so that it becomes closer to $3\sigma^*\alpha$. The next step is then relief of the Pauli repulsion by interaction (pushing down) of this antibonding combination by the empty $3\sigma^*\alpha$, which acts by the donor–acceptor interaction of the empty $3\sigma^*\alpha$ with the $\sigma(\mathrm{CH})\alpha$ part of the antibonding combination. The donor–acceptor interaction of $3\sigma^*\alpha$ with the ($\sigma(\mathrm{CH})\alpha$ part of the) bonding combination will be small due to the enhanced orbital energy gap.

In Figure 6a we give the orbital interaction diagram for the ^{5}**1** interaction with methane at the transition state geometry. The diagram is slightly idealized. In practice there is sometimes almost arbitrary mixing in of some orbitals (e.g., a π^* with an almost orthogonal σ type orbital), due to energetic proximity, but without much energetic consequence. For simplicity we only draw the main orbitals involved in the interaction, and the

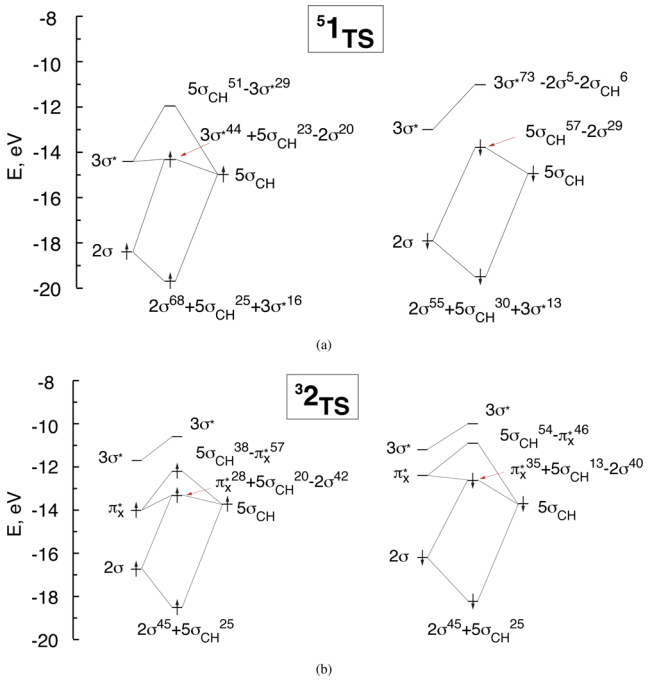

Figure 6. Transition state orbital interaction diagrams of selected fragment KS orbitals of the free quintet $FeO(H_2O)_5$ (**1**) (a) and triplet $FeO(H_2O)(NH_3)_4$ (**2**) (b) molecules, and the methane HOMO. All fragments are taken in the TS geometries. The methane HOMO was shifted by an amount estimated from the average shift of the noninteracting methane orbitals in the reactant complex. The compositions of the orbitals in terms of the fragment orbitals are given as superscripts.

percentages of the fragment orbitals written at those levels in the diagram actually represent the total amount of a fragment orbital in the set of nearby levels into which it may "arbitrarily" mix. The percentages of the fragment orbitals at the levels in the diagram add up to the totals, as depicted in Figure 4, for example. The diagrams show in the TS of ^{5}**1** a three-orbital interaction pattern in the α channel. The lengthening of the Fe–O bond in the TS is a simple consequence of the donation into the antibonding $3\sigma^*$ or equivalently can be viewed as lengthening of the bond in order to lower the antibonding $3\sigma^*$ so as to maximize its interaction with the lower-lying $\sigma(CH)\alpha$ orbital. In the ^{3}**2** system, the orbital interaction diagram given in Figure 6b shows in the β channel the involvement of $2\pi^*\beta$ instead of the $3\sigma^*$ in the electron transfer from substrate to oxidant. In the α manifold there is no net transfer of electron density out of $\sigma(CH)$. We note that the energetic effects of the orbital interactions as pictured in these diagrams represent the catalytic action of the oxidant in the breaking of the (strong) C–H bond as presented in Figure 2: whereas complete breaking of the C–H bond in methane would raise the energy by ca. 100 kcal/mol, the increasingly strong orbital interactions leading to formation of the O–H bond during the C–H dissociation lower the energy enormously and leave only a TS barrier of ca. 5 kcal/mol.

The interaction in the σ channel of $\sigma(CH)$ with $3\sigma^*$ is determined by the (KS Hamiltonian) interaction matrix element, which is judged by the overlap. This overlap is significant owing to a large O $2p_z$ contribution in the $3\sigma^*$. From the first detailed analyses[13] of the electronic structure of FeO^{2+} and $FeO(H_2O)_5^{2+}$ it has been apparent that both the occupied bonding (2σ) and unoccupied antibonding ($3\sigma^*$) orbitals are strong mixtures of Fe d_{z^2} and O $2p_z$, signifying covalent bonding. The Fe–O bond is not a simple coordinative bond of Fe with an oxo group but is a strong, short, covalent bond. Thus, although $3\sigma^*\alpha$ is expected to be Fe 3d type (in the common picture of ligand levels below metal d levels), it is well-known that $3\sigma^*\alpha$ actually has a large O $2p_z$ contribution, often higher than the Fe 3d content.[13,48,51] The precise percentages of Fe and O character vary between α and β spin and of course depend on the functional used. We do not find these percentages to vary much in the free reactants between the Fe–O bond length of the equilibrium and the TS geometry, as also observed in ref 27. For example, the B3LYP functional shows stronger changes of the composition of $3\sigma^*$ upon Fe–O bond stretching in comparison to nonhybrid functionals such as BLYP and BP86: going from RC to TS geometry in the free reactant, we find with BLYP an increase of O $2p_z$ character of $3\sigma^*\alpha$ from 34.5% to 37.2%, while with B3LYP it increases from 42.8% to 58%. However, it has been cautioned several times that B3LYP exhibits too extreme spin polarization ("broken-symmetry" type solutions), as judged by high-accuracy wave function calculations.[83−87] Because the Fe $3d_{z^2}$ content of $2\sigma\alpha$ and the O content of $3\sigma^*\alpha$ increase when the Fe–O bond is lengthened, it has been suggested that this situation might be pictured as a virtually broken σ bond between Fe and O, with a full α spin electron on Fe and a β spin electron on O: i.e., the formation of an oxyl radical ($O^{\bullet-}$) spin coupled to an Fe(III) ion.[51,54,64,65] In order to see if we can confirm this picture, we will investigate the electronic structure changes along the reaction coordinate more closely.

It should be noted that the iron–oxo bond lengthening to the transition state is quite modest (see Table 2), from ca. 1.621 Å in the free FeO^{2+} complexes to bond lengths in the

DOI: 10.1021/cs501721y
ACS Catal. 2015, 5, 1475–1488

Table 2. Iron−Oxo Bond Dissociation Energies (in kcal/mol) from the Equilibrium Geometry of the Free Oxidants (R) and from the Transition State Geometry (TS) and the Corresponding Bond Lengths r_{FeO} (in Å)[a]

	1				2			
	$S = 2$		$S = 1$		$S = 2$		$S = 1$	
	E	r_{FeO}	E	r_{FeO}	E	r_{FeO}	E	r_{FeO}
R	84	1.621	96	1.627	90	1.627	101	1.632
TS	78	1.728	88	1.665	83	1.755	95	1.761
ΔE	6.3		8.1		6.7		6.2	

[a]The energy difference $\Delta E = E(R) - E(TS)$ corresponds to the Fe−O bond elongation energy.

Table 3. Spin Densities ($\rho_\alpha - \rho_\beta$) on Oxo Oxygen, Iron, Iron−Oxo Moiety (FeO), and Methane Carbon and Mulliken Charges (Q) on O, Fe, and C in the Reactant Complex (RC) and Transition State (TS) Compounds[a]

Reactant Complexes (RC) and Transition States (TS)														
		RC							TS					
		$\rho_\alpha - \rho_\beta$				Q			$\rho_\alpha - \rho_\beta$				Q		
compd	spin	O	Fe	FeO	C	O	Fe	C	O	Fe	FeO	C	O	Fe	C
1	$S = 2$	0.67	3.16	3.83	−0.05	−0.41	1.85	0.80	0.42	3.78	4.20	−0.42	−0.50	1.78	0.67
	$S = 1$	0.89	1.11	2.00	0.01	−0.37	1.85	0.83	−0.03	2.36	2.34	−0.37	−0.48	1.73	0.69
2	$S = 2$	0.69	3.04	3.72	−0.01	−0.42	1.73	0.81	0.40	3.88	4.29	−0.62	−0.50	1.60	0.61
	$S = 1$	0.82	1.21	2.03	0.01	−0.41	1.97	0.85	0.43	0.97	1.39	0.63	−0.48	1.91	0.54
Free Reactants **1** and **2** at the RC or TS Geometry														
		RC					TS							
		$\rho_\alpha - \rho_\beta$			Q		$\rho_\alpha - \rho_\beta$				Q			
compd	spin	O	Fe	FeO	O	Fe	O	Fe	FeO		O	Fe		
1	$S = 2$	0.72	3.01	3.74	−0.34	1.86	0.72	3.04	3.76		−0.28	1.78		
	$S = 1$	0.89	1.13	2.03	−0.36	1.86	0.94	1.07	2.01		−0.29	1.76		
2	$S = 2$	0.71	2.98	3.69	−0.39	1.75	0.63	3.05	3.68		−0.32	1.59		
	$S = 1$	0.83	1.20	2.04	−0.41	1.95	0.88	1.17	2.05		−0.37	1.90		

[a]The corresponding values for the free oxidant at the reactant complex (RC) and the transition state (TS) geometries are also shown.

transition states ranging in the aquo complexes from 1.665 Å (^{3}**1** TS) to 1.728 Å (^{5}**1** TS), and in the ammoniated complexes from 1.755 Å (^{5}**2** TS) to 1.761 Å (^{3}**2** TS). These small bond elongations do not entail significant changes in the iron−oxo bond strengths: whereas the Fe−O bond energies for these complexes are in the range of 80−100 kcal/mol (much stronger than typical coordinative bonds), the weakening of these strong bonds to the TS amounts to only ca. 6 kcal/mol (see Table 2). The Fe−O bond is by no means broken in the TS. The spin densities on Fe and O also do not change significantly (in the free oxidants) when one elongates the Fe−O bond to the TS length, as can be seen in Table 3. In this table the spin densities in the reactant complex and the transition state are given, and also the spin densities in the free oxidants (both the $[FeO(H_2O)_5]^{2+}$ complex **1** and the $[FeO(H_2O)(NH_3)_4]^{2+}$ complex **2**) in the geometries these systems have in the reactant complexes (RC) and the transition states (TS), but without methane being present. The TS geometries are characterized by the Fe−O bond lengthenings mentioned before. It is clear that the spin densities on O and Fe change, in the isolated reactants, very little upon the rather small bond lengthening to the TS. This geometry change does not induce significant change in the electronic structure; there is no indication of the breaking of an Fe−O bond or a significant change in the radical character of O. The changes in spin density are more pronounced upon interaction with methane in the TS due to the transfer of electronic charge and spin density taking place from methane to FeO. This is clear from the negative spin densities that build up on the C atom in the TS and the increase of spin-up density on FeO in ^{5}**1** and ^{5}**2**. In ^{3}**2** β spin density is transferred via the π^* channel, and we see accordingly in Table 3 in the TS considerable net α spin density on C and a decrease of the α spin density on FeO. In ^{3}**1** the interaction with methane in the TS causes the switch of an electron from $\pi^*\alpha$ to $d_{x^2-y^2}\alpha$, with strong reduction of the α spin density on O and increase of α spin density on Fe. In addition the transfer of α spin density from methane to FeO (via the $\pi\alpha$ channel) leads in this case again to negative spin density on C and net increase of the α spin density on FeO. There is also some reorganization of the orbitals on the FeO moiety, to the effect that the increase of α spin density on FeO in ^{5}**1** and ^{5}**2** is on Fe rather than on O, while the β density increase (lowering of α density) in ^{3}**2** is more on O. In the case of ^{3}**1** (again, a rather special case) one should first do the switch from $\pi^*\alpha$ to $d_{x^2-y^2}\alpha$, and after that point the increase of α density in the transfer from methane proves to be to both Fe and O.

The evolution of the spin density along the complete reaction path is shown in Figures 7 and 8 (spin density is plotted against the intrinsic reaction coordinate, projected on the O−H distance before the TS and on the C−H distance after the TS). The clearest development in spin density is on the C atom, where the spin density develops from 0 in the free reactant to ca. −0.8 in the systems where an α electron is transferred (all systems except ^{3}**2**). In ^{3}**2** (Figure 8b) a β electron is transferred, and the spin density on C develops from 0 to ca. +0.8. We have already seen that in ^{3}**1** we do not have, as in ^{3}**2**, a $\pi^*\beta$ channel, but an alternative route prevails, where a

DOI: 10.1021/cs501721y
ACS Catal. 2015, 5, 1475−1488

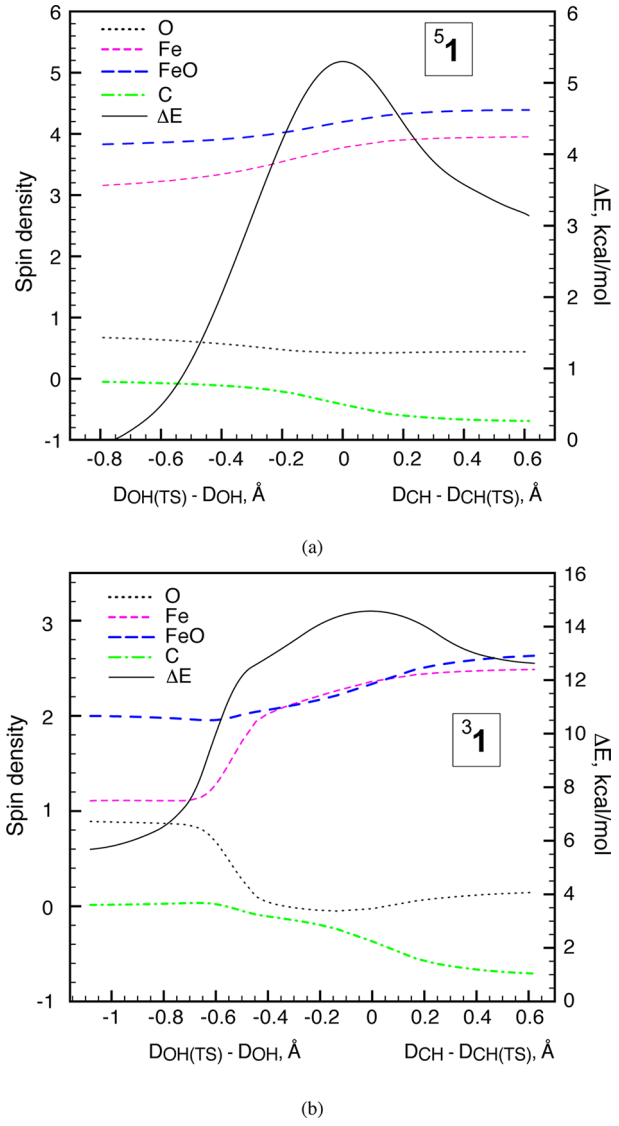

Figure 7. Spin density evolutions along the reaction coordinate in H abstraction from methane by $[FeO(H_2O)_5]^{2+}$ (**1**) in quintet (a) and triplet (b) states. The energy is shown by the black solid line with the values given on the secondary axis (maximum at the TS). The results were obtained along the intrinsic reaction coordinate (IRC) and are plotted along the projection of the IRC on the O−H coordinate before the TS and on the C−H coordinate after the TS.

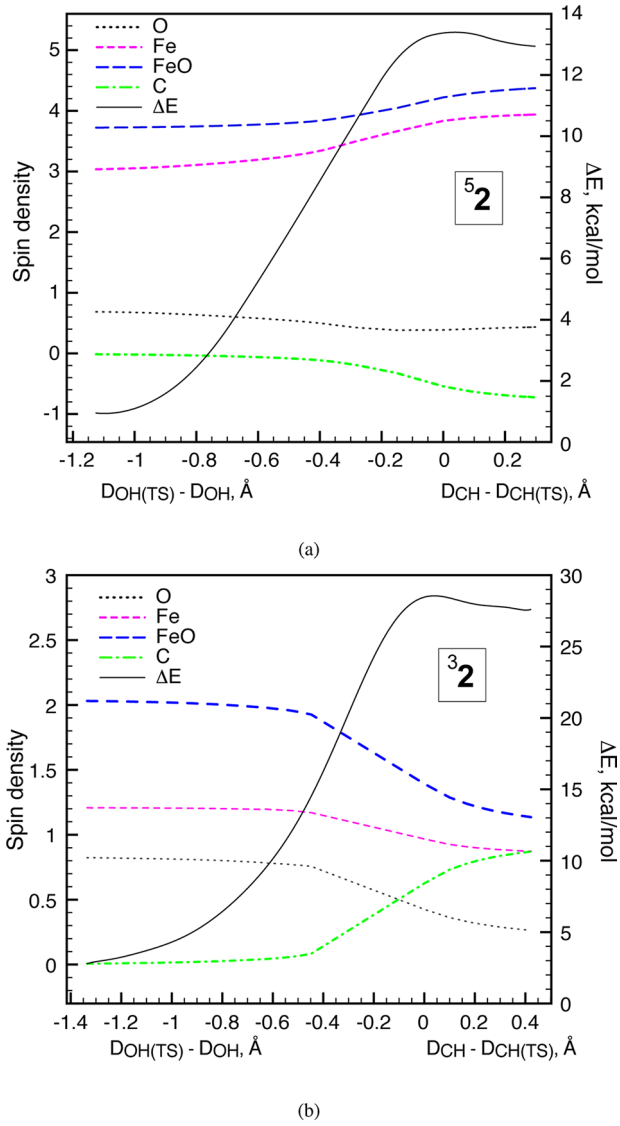

Figure 8. Spin density evolutions along the reaction coordinate in H abstraction from methane by $[FeO(H_2O)(NH_3)_4]^{2+}$ (**2**) in quintet (a) and triplet (b) states. The energy is shown by the black solid line with the values given on the secondary axis (maximum at TS). The results were obtained along the intrinsic reaction coordinate (IRC), plotted along the projection of the IRC on the O−H coordinate before the TS and on the C−H coordinate after the TS.

$\pi^*\alpha$ electron is excited to $d_{x^2-y^2}$ and then an α electron is transferred from $\sigma(CH)\alpha$ to $\pi^*\alpha$. Therefore, one can only see in ^{3}**2** (Figure 8b) β spin density develop on the C atom. The most important observation in Figures 7 and 8 is the very gradual changes in the spin densities on O and Fe. In particular in the quintet systems ^{5}**1** and ^{5}**2** the spin densities change slowly all along the reaction coordinate. The only case where there are clear changes in spin density on O and Fe is in ^{3}**1** (Figure 7b), where a visible reduction of α spin density on O occurs already before the TS, with a simultaneous increase on Fe. However, this is due to the mentioned special circumstance in this case that an α spin electron switches from the $\pi^*\alpha$ to the predominantly Fe $d_{x^2-y^2}\alpha$ orbital. In ^{3}**2** (Figure 8b) there is again only smooth change in the O spin density, which only becomes sizable when the total FeO spin density changes because of the donation out of the $\sigma\beta$(CH) bond orbital: cf. the increasing α spin density on C.

These electronic structure investigations do not support an oxyl radical picture of the ironoxo reactivity. We also note that the description of spin states in terms of a Heisenberg type spin coupling model is usually applied to situations where the energy difference between the spin states is small (on the order of 0.1 eV) and the overlap between the magnetic orbitals (which would here be Fe d_{z^2} and O $2p_z$) is so weak that the energy gap between the bonding and antibonding pair of orbitals is very small. In the present case the energy gap between 2σ and $3\sigma^*$ is large (on the order of 4 eV) and these AOs overlap considerably (cf. the contour plot in Figure 5 in ref 48 and the $3\sigma^*$ pictures in Figure 3). In summary, the present findings afford a straightforward orbital interaction interpretation of the hydrogen atom abstraction reaction by the $Fe^{IV}O^{2+}$ metal−oxo compound.

DOI: 10.1021/cs501721y
ACS Catal. 2015, 5, 1475−1488

CONCLUSIONS

The purpose of the present work is to highlight the ligand effects on the reactivity of the $Fe^{IV}O^{2+}$ group. Given the fact that the reactivity is determined by low-lying empty electron acceptor orbitals (EAO) on the FeO^{2+} receiving electrons donated by an occupied CH bonding orbital of methane (the electron donating orbital, EDO), it is clear that all factors which diminish the energy gap between these frontier orbitals will facilitate the reaction. At the CH_4 side, the most important factor is the lengthening of the reacting C−H bond along the reaction coordinate: the longer the bond, the less stable the CH bonding orbital and the more readily the interaction of this EDO with the EAO. This is the crucial energy-lowering interaction that counteracts the energy rise due to the lengthening and eventually the breaking of the C−H bond (see Figure 2 and see ref 50 for a more detailed discussion). At the FeO^{2+} side there are several factors. These are all related to the strength of the ligand field of the coordinated groups. The factor that has received the most interest is the importance of the spin state. It has been recognized[27,42,45,48,52,56−58,63,64,75,76,88−92] that the high-spin state is favorable, yielding lower transition barriers in comparison to the low-spin state. This can be understood from the lower orbital energy of the majority spin (conventionally taken to be α) acceptor frontier orbital caused by the stabilizing exchange field of an excess of unpaired electrons (there are four unpaired spins in the quintet vs only two in the triplet). In addition the EER principle emphasizes that transfer of a majority spin electron from the EDO to the EAO is favorable (will have a lower barrier) because there will be more stabilizing exchange interactions between the electrons.[61−63] The triplet state ^{3}**2**, with two unpaired α electrons, is less favorable because the acceptor orbital is in this case not a majority spin orbital, thus lacking the stabilization of the orbital energy by the exchange field. Moreover in this case a minority spin (β) electron is transferred (at least in our ammoniated model complex, or in the analogous P450 Cpd I system) (EER argument). Thus, these triplet states are unfavorable in terms of the frontier orbital picture (because the β acceptor orbital does not benefit from a specially low orbital energy, as the majority spin levels do) and according to the EER principle (because the incoming β electron does not have favorable exchange interaction with the existing unpaired α electrons). This has made it understandable that the TS barrier is typically higher on the triplet surface.

However, the ligand field that induces a low-spin configuration (a strong field) also affects the barrier in other ways. We have stressed the direct ligand effects, originating from the greater "pushing up" of the metal orbitals by strong ligands, which would make the energy of the FeO^{2+}-based EAO higher: i.e., less favorable. There is also an indirect charge effect of strong ligands: they donate more electronic charge to the metal and therefore move up all metal-based levels because of the less positive gross charge on the metal. The strong ligands that induce a triplet state will inevitably also have these other adverse effects. We have tried to quantify the bare spin effect and the (other) ligand effects for our model systems **1** and **2**. It appears that the ligand effect is even somewhat larger than the spin effect. We have concentrated here on the equatorial ligands; the same considerations apply to the trans axial ligand, where the direct pushing up effect of an axial lone pair on the σ^* acceptor orbital is relatively important[42] because the d_{z^2} character of σ^* implies that it has a pronounced lobe along the z axis.

Clearly, when one considers the difference between triplet and quintet reactivities within the same ligand environment, there are no added ligand effects. However, when one considers the general question of choosing a suitable ligand environment to enhance the reactivity of a (synthetic) metal−oxo compound, then these factors should be taken into account. We can summarize our findings in the following rules. (i) A high-spin state is advantageous both from a frontier orbital point of view and on account of the EER principle. A high-spin state occurs typically with a weak ligand field. (ii) A weak ligand field is favorable because it does not unduly push up the empty acceptor orbital, as strong ligands do, either directly (by orbital overlap) or indirectly (by bringing negative charge onto the metal). (iii) A strong equatorial ligand field simultaneously has two unfavorable effects: (a) pushing up the EAO (both directly by antibonding interaction between overlapping metal and ligand orbitals and indirectly by charge effect) and (b) inducing a low-spin state, with less exchange stabilization of the majority spin EAO. A strong axial ligand (*trans* to the oxo group) is unfavorable because of pushing up of the EAO mostly by orbital interaction (see ref 42). (iv) 3d transition metals have considerably more tight d orbitals than the metals from the second and third transition series. Since the more diffuse orbitals of the heavier transition metals make them more sensitive to the ligand field effects, it appears advantageous to use first-row transition metals. (v) Not only charging effects from the coordinative bonding but also of course overall charge by itself is very important: positive overall charge is favorable, since it stabilizes the EAO.[66] Note however that solvent effects also exert a strong influence on the EAO−EDO gap, which depends on the (sign of the) total charge.[79]

All of these considerations point to complexes of FeO^{2+} as favorable (first row metal), with ligands that coordinate through e.g. oxygen rather than through nitrogen and that preferably have a positive charge. Complexes of EDTA have been investigated as a possible realization of these desirable features.[66,79,93] Obviously, the present considerations are qualitative, and individual cases need to be studied with care. A more comprehensive theory would take into account σ and π characteristics of the ligands, which are obviously relevant not only for the porphyrin ligand but also for popular ligands such as the heterocyclic bases pyridine, imidazole, and benzimidazole.

ASSOCIATED CONTENT

Supporting Information

The following file is available free of charge on the ACS Publications website at DOI: 10.1021/cs501721y.

Energies of the frontier orbitals of the various systems (^{5}**1**, ^{3}**1**, ^{5}**2**, ^{3}**2**) and methane at the respective complex geometries (of reactant complexes, transition states, and for constrained linear approaches of methane) and a discussion of energy decomposition results (PDF)

AUTHOR INFORMATION

Corresponding Author

*E-mail for E.J.B.: E.J.Baerends@vu.nl.

Notes

The authors declare no competing financial interest.

DOI: 10.1021/cs501721y
ACS Catal. 2015, 5, 1475−1488

■ ACKNOWLEDGMENTS

We thank the National Research School Combination "Catalysis by Design" for financial support and The Netherlands Foundation for Scientific Research (NWO) for computer time.

■ REFERENCES

(1) Schöneboom, J. C.; Cohen, S.; Lin, H.; Shaik, S.; Thiel, W. *J. Am. Chem. Soc.* **2004**, 4017−4034.
(2) Meunier, B.; de Visser, S. P.; Shaik, S. *Chem. Rev.* **2004**, *104*, 3947−80.
(3) Price, J. C.; Barr, E. W.; Tirupati, B.; Bollinger, J. M.; Krebs, C. *Biochemistry* **2003**, *42*, 7497−508.
(4) Hoffart, L. M.; Barr, E. W.; Guyer, R. B.; Bollinger, J. M.; Krebs, C. *Proc. Natl. Acad. Sci. U.S.A.* **2006**, *103*, 14738−43.
(5) Shu, L.; Nesheim, J. C.; Kauffmann, K.; Münck, E.; Lipscomb, J. D.; Que, L. *Science* **1997**, *275*, 515−518.
(6) Solomon, E. I.; Sundaram, U. M.; Machonkin, T. E. *Chem. Rev.* **1996**, *96*, 2563−2606.
(7) Que, L. J.; Dong, Y. *Acc. Chem. Res.* **1996**, *29*, 190−196.
(8) Bray, W. C.; Gorin, M. H. *J. Am. Chem. Soc.* **1932**, *54*, 2124−2125.
(9) Groves, J. T.; McClusky, G. A. *J. Am. Chem. Soc.* **1976**, *98*, 859−861.
(10) Groves, J. T.; Van der Puy, M. *J. Am. Chem. Soc.* **1976**, *98*, 5290−5297.
(11) Buda, F.; Ensing, B.; Gribnau, M. C. M.; Jan, E. *Chem. Eur. J.* **2001**, 2775−2783.
(12) Ensing, B.; Buda, F.; Blöchl, P. E.; Baerends, E. J. *Phys. Chem. Chem. Phys.* **2002**, *4*, 3619−3627.
(13) Buda, F.; Ensing, B.; Gribnau, M. C. M.; Baerends, E. J. *Chem. Eur. J.* **2003**, *9*, 3436−44.
(14) Kremer, M. L. *J. Phys. Chem. A* **2003**, *107*, 1734−1741.
(15) Ensing, B.; Buda, F.; Gribnau, M. C. M.; Baerends, E. J. *J. Am. Chem. Soc.* **2004**, *126*, 4355−4365.
(16) Yamamoto, N.; Koga, N.; Nagaoka, M. *J. Phys. Chem. B* **2012**, *116*, 14178−82.
(17) Green, M. T.; Dawson, J. H.; Gray, H. B. *Science* **2004**, *304*, 1653−6.
(18) Groves, J. T. *J. Inorg. Biochem.* **2006**, *100*, 434−47.
(19) Rittle, J.; Green, M. T. *Science* **2010**, *330*, 933−7.
(20) Schöneboom, J. C.; Neese, F.; Thiel, W. *J. Am. Chem. Soc.* **2005**, *127*, 5840−53.
(21) Shaik, S.; Kumar, D.; de Visser, S. P.; Altun, A.; Thiel, W. *Chem. Rev.* **2005**, *105*, 2279−328.
(22) de Visser, S. P.; Tahsini, L.; Nam, W. *Chemistry* **2009**, *15*, 5577−87.
(23) Tahsini, L.; Bagherzadeh, M.; Nam, W.; de Visser, S. P. *Inorg. Chem.* **2009**, *48*, 6661−9.
(24) Altun, A.; Shaik, S.; Thiel, W. *J. Am. Chem. Soc.* **2007**, *129*, 8978−87.
(25) Hazan, C.; Kumar, D.; de Visser, S. P.; Shaik, S. *Eur. J. Inorg. Chem.* **2007**, *2007*, 2966−2974.
(26) Chen, H.; Lai, W.; Shaik, S. *J. Phys. Chem. B* **2011**, *115*, 1727−1742.
(27) Rosa, A.; Ricciardi, G. *Inorg. Chem.* **2012**, *51*, 9833−45.
(28) Rosenzweig, A. C.; Nordlund, P.; Takahara, P. M.; Frederick, C. A.; Lippard, S. J. *Chem. Biol.* **1995**, *2*, 409−418.
(29) Solomon, E. I.; Brunold, T. C.; Davis, M. I.; Kemsley, J. N.; Lee, S. K.; Lehnert, N.; Neese, F.; Skulan, A. J.; Yang, Y. S.; Zhou, J. *Chem. Rev.* **2000**, *100*, 235−350.
(30) Merkx, M.; Kopp, D. A.; Sazinsky, M. H.; Blazyk, J. L.; Müller, J.; Lippard, S. J. *Angew. Chem., Int. Ed.* **2001**, *40*, 2782−2807.
(31) Kopp, D. A.; Lippard, S. J. *Curr. Opin. Chem.Biol.* **2002**, *6*, 568−576.
(32) Yoon, S.; Lippard, S. J. *J. Am. Chem. Soc.* **2004**, *126*, 16692−16693.
(33) Xue, G.; Wang, D.; De Hont, R.; Fiedler, A. T.; Shan, X.; Münck, E.; Que, L. *Proc. Natl. Acad. Sci. U.S.A.* **2007**, *104*, 20713−20718.
(34) Kovaleva, E. G.; Neibergall, M. B.; Chakrabarty, S.; Lipscomb, J. D. *Acc. Chem. Res.* **2007**, *40*, 475−483.
(35) Wang, D.; Farquhar, E. R.; Stubna, A.; Münck, E.; Que, L. *Nat. Chem.* **2009**, *1*, 145−150.
(36) Tinberg, C. E.; Lippard, S. J. *Acc. Chem. Res.* **2011**, *44*, 280−288.
(37) Panay, A. J.; Lee, M.; Krebs, C.; Bollinger, J. M.; Fitzpatrick, P. F. *Biochemistry* **2011**, DOI: 10.1021/bi1019868.
(38) Nam, W. *Acc. Chem. Res.* **2007**, *40*, 522−531.
(39) Lyakin, O. Y.; Shteinman, a. a. *Kinet. Catal.* **2012**, *53*, 694−713.
(40) McDonald, A. R.; Que, L. *Coord. Chem. Rev.* **2012**, *257*, 414−428.
(41) Neese, F. *J. Inorg. Biochem.* **2006**, *100*, 716−726.
(42) Bernasconi, L.; Louwerse, M. J.; Baerends, E. J. *Eur. J. Inorg. Chem.* **2007**, 3023−3033.
(43) Pestovsky, O.; Stoian, S.; Bominaar, E. L.; Shan, X.; Münck, E.; Que, L.; Bakac, A. *Angew. Chem., Int. Ed.* **2005**, *117*, 7031−7034.
(44) Decker, A.; Clay, M. D.; Solomon, E. I. *J. Inorg. Biochem.* **2006**, *100*, 697−706.
(45) Decker, A.; Rohde, J. U.; Klinker, E. J.; Wong, S. D.; Que, L., Jr.; Solomon, E. I. *J. Am. Chem. Soc.* **2007**, *129*, 15983−15996.
(46) de Visser, S. P. *J. Am. Chem. Soc.* **2006**, *128*, 15809−15818.
(47) de Visser, S. P. *J. Am. Chem. Soc.* **2006**, *128*, 9813−24.
(48) Louwerse, M. J.; Baerends, E. J. *Phys. Chem. Chem. Phys.* **2007**, *9*, 156−66.
(49) Michel, C.; Baerends, E. J. *Inorg. Chem.* **2009**, *48*, 3628−38.
(50) Gopakumar, G.; Belanzoni, P.; Baerends, E. J. *Inorg. Chem.* **2012**, *51*, 63−75.
(51) Neidig, M. L.; Decker, A.; Choroba, O. W.; Huang, F.; Kavana, M.; Moran, G. R.; Spencer, J. B.; Solomon, E. I. *Proc. Natl. Acad. Sci. U. S. A.* **2006**, *103*, 12966.
(52) Geng, C.; Ye, S.; Neese, F. *Angew. Chem., Int. Ed.* **2010**, *49*, 5717−20.
(53) Decker, A.; Rohde, J. U.; Klinker, E. J.; Wong, S. D.; Que, L., Jr.; Solomon, E. I. *J. Am. Chem. Soc.* **2007**, *129*, 15983−15996.
(54) Srnec, M.; Wong, S. D.; England, J.; Que, L.; Solomon, E. I. *Proc. Natl. Acad. Sci. U.S.A.* **2012**, *109*, 14326.
(55) Sun, X.; Geng, C.; Huo, R.; Ryde, U.; Bu, Y.; Li, J. *J. Phys. Chem. B* **2014**, *118*, 1493−1500.
(56) Shaik, S.; Filatov, M.; Schröder, D.; Schwarz, H. *Chem. Eur. J.* **1998**, *4*, 193−199.
(57) Hirao, H.; Kumar, D.; Que, L., Jr; Shaik, S. *J. Am. Chem. Soc.* **2006**, *128*, 8590−8606.
(58) Shaik, S.; Hirao, H.; Kumar, D. *Acc. Chem. Res.* **2007**, *40*, 532−542.
(59) Sastri, C. V.; Lee, J.; Oh, K.; Lee, Y. J.; Lee, J.; Jackson, T. A.; Ray, K.; Hirao, H.; Shin, W.; Halfen, J. A.; et al. *Proc. Natl. Acad. Sci. U.S.A.* **2007**, *104*, 19181−6.
(60) Hirao, H.; Que, L., Jr; Nam, W.; Shaik, S. *Chem. Eur. J.* **2008**, *14*, 1740−1756.
(61) Janardanan, D.; Wang, Y.; Schyman, P.; Que, L., Jr.; Shaik, S. *Angew. Chem., Int. Ed.* **2010**, *122*, 3342−3345.
(62) Chen, H.; Lai, W.; Shaik, S. *J. Phys. Chem. Lett.* **2010**, *1*, 1533−1540.
(63) Shaik, S.; Chen, H.; Janardanan, D. *Nat. Chem.* **2011**, *3*, 19−27.
(64) Ye, S.; Neese, F. *Curr. Opin. Chem. Biol.* **2009**, *13*, 89−98.
(65) Ye, S.; Neese, F. *Proc. Natl. Acad. Sci. U.S.A.* **2011**, *108*, 1228−1233.
(66) Bernasconi, L.; Baerends, E. J. *Eur. J. Inorg. Chem.* **2008**, *2008*, 1672−1681.
(67) *ADF 2010.01*; SCM, Theoretical Chemistry, Vrije Universiteit Amsterdam, Amsterdam, The Netherlands, 2010; http://www.scm.com.
(68) Baerends, E.; Ellis, D.; Ros, P. *Chem. Phys.* **1973**, *2*, 41−51.
(69) Fonseca Guerra, C.; Snijders, J.; Te Velde, G.; Baerends, E. *Theor. Chem. Acc.* **1998**, *99*, 391−403.

DOI: 10.1021/cs501721y
ACS Catal. 2015, 5, 1475−1488

(70) van Lenthe, E.; Baerends, E.; Snijders, J. *J. Chem. Phys.* **1994**, *101*, 9783.
(71) Becke, A. *Phys. Rev. A* **1988**, *38*, 3098.
(72) Lee, C.; Yang, W.; Parr, R. *Phys. Rev. B* **1988**, *37*, 785.
(73) Becke, A. *J. Chem. Phys.* **1993**, *98*, 5648.
(74) Que, L. *Acc. Chem. Res.* **2007**, *40*, 493−500.
(75) Kumar, D.; Hirao, H.; Que, L., Jr.; Shaik, S. *J. Am. Chem. Soc.* **2005**, *127*, 8026−8027.
(76) Rosa, A.; Ricciardi, G.; Baerends, E. J. *Inorg. Chem.* **2010**, *49*, 3866−3880.
(77) Tang, H.; Guan, J.; Zhang, L.; Liu, H.; Huang, X. *Phys. Chem. Chem. Phys.* **2012**, *14*, 12863−74.
(78) Tang, H.; Guan, J.; Liu, H.; Huang, X. *Inorg. Chem.* **2013**, *52*, 2684−2696.
(79) Bernasconi, L.; Baerends, E. J. *J. Am. Chem. Soc.* **2013**, *135*, 8857−8867.
(80) Ye, S.; Geng, C.-Y.; Shaik, S.; Neese, F. *Phys. Chem. Chem. Phys.* **2013**, *15*, 8017−30.
(81) Shaik, S.; Cohen, S.; Wang, Y.; Chen, H.; Kumar, D.; Thiel, W. *Chem. Rev.* **2010**, *110*, 949−1017.
(82) Dietl, N.; Schlangen, M.; Schwarz, H. *Angew. Chem., Int. Ed.* **2012**, *51*, 5544−5555.
(83) Reiher, M.; Salomon, O.; Artur Hess, B. *Theor. Chem. Acc.* **2001**, *107*, 48−55.
(84) Conradie, J.; Ghosh, A. *J. Phys. Chem. B* **2007**, *111*, 12621−4.
(85) Swart, M. *J. Chem. Theor. Comp.* **2008**, *4*, 2057−2066.
(86) Boguslawski, K.; Jacob, C. R.; Reiher, M. *J. Chem. Theor. Comput.* **2011**, 2740−2752.
(87) Radon, M.; Broclawik, E.; Pierloot, K. *J. Phys. Chem. B* **2010**, *114*, 1518−28.
(88) Hirao, H.; Kumar, D.; Thiel, W.; Shaik, S. *J. Am. Chem. Soc.* **2005**, *127*, 13007−18.
(89) Johansson, A. J.; Blomberg, M. R. A.; Siegbahn, P. E. M. *J. Phys. Chem. C* **2007**, *111*, 12397−12406.
(90) Comba, P.; Maurer, M.; Vadivelu, P. *Inorg. Chem.* **2009**, *48*, 10389−96.
(91) Comba, P.; Wunderlich, S. *Chemistry* **2010**, *16*, 7293−9.
(92) Jaccob, M.; Comba, P.; Maurer, M.; Vadivelu, P.; Venuvanalingam, P. *Dalton Trans.* **2011**, *40*, 11276−81.
(93) Bernasconi, L.; Baerends, E. J. *Inorg. Chem.* **2009**, *48*, 527−40.
(94) It should be noted that in the methane hydroxylation reaction the H abstraction is the first part of the reaction, followed by the O rebound. Therefore, the conventional notation for the H abstraction product is IN (intermediate). Nevertheless, we denote the complex as PC, since we focus on the H abstraction reaction throughout the paper.

DOI: 10.1021/cs501721y
ACS Catal. 2015, 5, 1475−1488